Available online at www.sciencedirect.com

ScienceDirect

Procedia Engineering 62 (2013) 422 – 431

Procedia Engineering

www.elsevier.com/locate/procedia

The 9th Asia-Oceania Symposium on Fire Science and Technology

A model to predict carbon monoxide of woods under external heat flux – Part II: Validation and application

Long Shi*, Michael Yit Lin Chew

Department of Building, National University of Singapore, Singapore, 117566

Abstract

A model to predict carbon monoxide (CO) of woods under external heat flux was developed. To improve the modeling accuracy, fire processes such as water evaporation, volume shrinkage, water and gas transport inside wood slab were considered. Three reactions such as water evaporation, oxidation reactions of virgin wood and char were included. Temperature and moisture dependent thermal properties were used for modeling input. In the second part of this study, this model was validated by experiments. Comparisons between modeling and experiments showed that mass loss rate and CO release rate can be well predicted for woods under different moisture contents and external heat flux. Volume shrinkage, transport processes of water and gas volatiles inside wood slab were also included.

This paper serves as validation and application of a mathematical model in Part I: Theory of a model to predict CO of woods under external heat flux. This model intends to provide a practical tool to predict toxic gases of combustible materials under fire conditions.

Keywords: Wood; Carbon monoxide; Toxic gas; Water evaporation; Shrinkage; Mass transport

1. Introduction

Two types of ignition methods were used in cone calorimeter previously. Kindle ignition [1] means combustible materials are ignited by external heat sources such as flame, sparks or hot surface, and in general, measurement of ignition point based on the ASTM International is widely used. Autoignition [2-3] means combustible materials are ignited as a result of internal heating, which arises spontaneously if there is an exothermic process liberating heat faster than it can be lost to the surrounding.

Autoignition is a complex phenomenon. Blijderveen et al. [4] obtained that autoignition behavior is determined by a combination of convective heat transfer between primary air flow and fuel bed and heat gained by reactions in the fuel bed. Wang et al. [5] analyzed the influence of ambient pressure and oxygen content on autoignition by conducting contrastive experiments at two different altitudes. Tahsini and Farshchi [6] studied the autoignition of polymer numerically and experimentally to analyze its controlling parameters.

For validation of this model, experiments of woods under external heat flux were taken by autoignition in a cone calorimeter, which means spark plug wasn't used during whole experimental time. This two-part study provides theory, validation and application of a one-dimensional model used to predict carbon monoxide (CO) of woods under external heat flux. Part I of this study has shown the theory of this mathematical model, including water evaporation, volume shrinkage, transport processes of liquids and gas volatiles inside a wood slab. Temperature and moisture dependent thermal properties were used for modeling input. Comparisons between modeling and experiments will be taken in the following contents.

* Corresponding author. Tel.: +65 8381 8700.
E-mail address: shilong@mail.ustc.edu.cn; shilong@nus.edu.sg.

doi:10.1016/j.proeng.2013.08.084

2. Experiments

2.1. Materials

Wood samples used in experiments were American cherry with average density is 558 kg/m^3. The sample sizes are 100 mm × 100 mm with different thicknesses, such as 10 mm and 20 mm. Samples were put under ambient environment for more than 24 hours. Moisture contents of wood samples were then measured according to the oven dry method [7] by a chamber furnace. In the furnace, temperature inside kept at a range of 102 to 105 °C to drive off the water. Periodical re-weighing were taken until no further weight loss was registered. The moisture content (wet basis) of woods samples was then obtained. The average moisture content of tested samples is about 0.11.

2.2. Apparatus

Cone calorimeter as a frequent used equipment for piloted and autoignition experiments was used in this study [8]. Wood samples were put in horizontal orientation on specimen holder. External heat fluxes of 25, 50, and 75 kW/m^2 were chosen for this study, representing the low, middle and high external heat flux. Fig. 1 shows a view of wood sample in cone calorimeter.

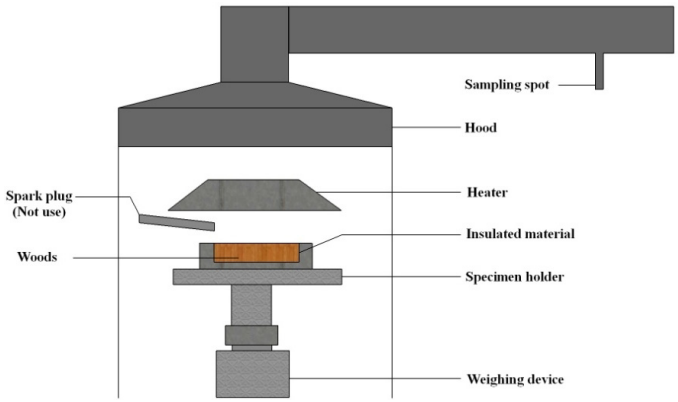

Fig. 1. A view of wood sample in cone calorimeter.

2.3. Procedure

Before experiments, gas analyzers and external heat flux were first calibrated accordingly. Wood samples were then secured on a specimen holder and placed under the heater horizontally. The edges and rear surface of the wood samples were covered with aluminum foil for insulation. Change in weight was dynamically recorded using the build-in weighting device. Spark plug was not used during whole experimental time.

3. Comparison with experiments

3.1. Mass loss rate

Noises were produced during experiments in mass loss history data. Savitzky-Golay method [9-10] was used to solve this problem. This method optimally fits a set of data points to a polynomial in the least-squares sense, which has been developed and generalized well in the literatures. The main advantage of this method is that it tends to preserve features of the distribution such as relative maxima, minima and width.

Figure 2 shows comparisons of mass loss rate (MLR) between predictions and experiments of wood samples under 25 kW/m^2 external heat flux. From both the prediction and experiments, three stages of mass loss can be observed. The first is the water evaporation. When temperature of a wood slice is higher than 100 °C, liquid water start to evaporate as more heat is absorbed. Water evaporation process can be observed obviously by MLR history data under this external heat flux. The second stage is the preliminary pyrolysis reaction of virgin wood. This stage begins when woods start to decompose, may be

when temperature is higher than 240 °C [11]. The third stage is the pyrolysis reactions of both virgin wood and char. Peak MLR can be observed in this stage.

Observation of water evaporation process is much obvious from prediction than experiment. The reason why the water evaporation process isn't obvious may be because the time period of evaporation process is short and water takes a small part of whole solid phase. In this case, mass loss is hard to be measured in such a short time. Another reason may be that some jump points in MLR data are ignored after smoothing.

From the figure, it is noticed that peak MLR happens earlier and increases a lot with thin samples. This is because absorbed heat per unit mass increase for thin samples under same external heat flux, and because heat is easier to penetrate into depth.

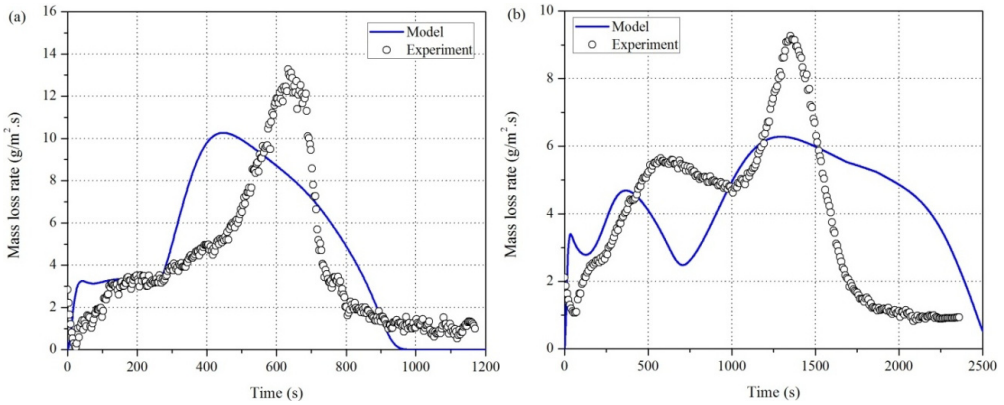

Fig. 2. Comparisons of MLR between prediction and experiment under 25 kW/m^2 heat flux for: (a) 10 mm thickness and (b) 20 mm thickness.

Figure 3 shows comparisons of MLR between predictions and experiments under 50 kW/m^2 external heat flux. It is noticed that modeling results obey very well with experimental data. As mentioned above, three mass loss stages can be observed when wood samples are put under low external heat flux. However, the first stage under middle external heat flux is difficult to be identified. Prediction shows a tiny peak at the very beginning. This may be because that the first two stages are very close, and the time interval between the start of water evaporation and pyrolysis reaction of virgin wood is small. As shown above, peak MLR of second stage were predicted a little earlier than experimental data for 10 mm thickness sample. For 20 mm thickness sample, an opposite phenomenon can be observed. This phenomenon may be due to the kinetic data for pyrolysis reaction of wood char.

Figure 4 shows comparisons of MLR of wood samples between predictions and experiments under 75 kW/m^2 external heat flux. It is noticed that the prediction fits very well with experimental data. This indicated that fire behaviors of wood samples under higher heat flux also can be well predicted by this model.

From the comparisons of MLR between predictions and experiments, it is noticed that this model can predict MLR of wet woods under different external heat flux well. The characteristics of MLR for wood samples with different thicknesses can be also well predicted.

3.2. CO release rate

Experiments were taken without use of sparkplug during whole experimental time. When wood samples were positioned under 25 kW/m^2, no visible flame was observed during the whole experimental period. It is considered that wood samples haven't been ignited under this external heat flux. It presents that the wood samples go through smoldering combustion under this external heat flux. For external heat flux of 50 and 75 kW/m^2, wood samples were ignited as visible flame was observed. The details about the experimental results can be seen elsewhere [2].

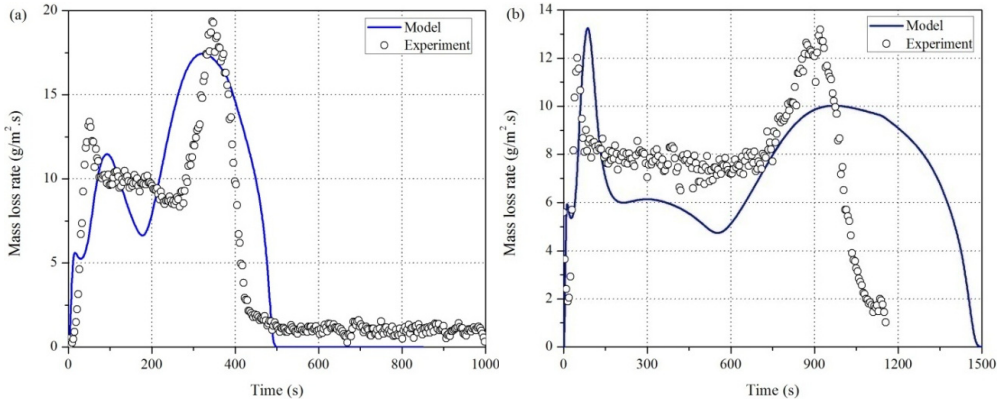

Fig. 3. Comparisons of MLR between prediction and experiment under 50 kW/m^2 heat flux for: (a) 10 mm thickness and (b) 20 mm thickness.

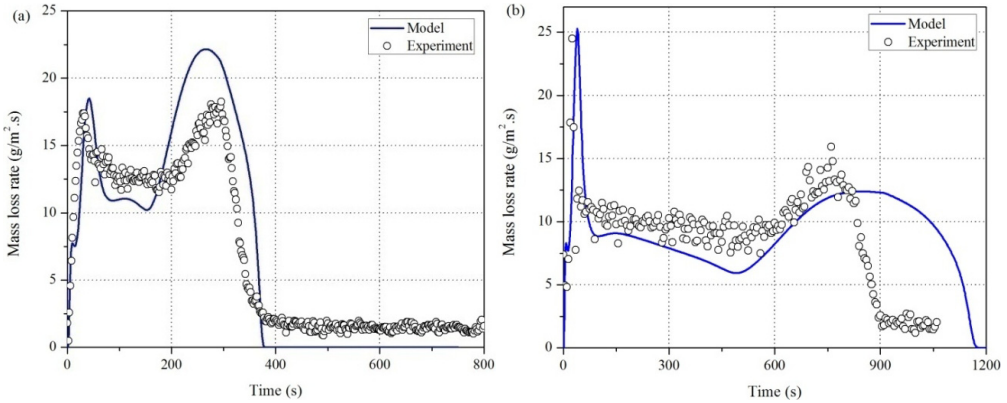

Fig. 4. Comparisons of MLR between prediction and experiment under 75 kW/m^2 heat flux for: (a) 10 mm thickness and (b) 20 mm thickness.

Figure 5 shows comparisons of CO release rate between predictions and experiments under 25 kW/m^2 external heat flux. It is noticed that the CO release rate for 20 mm thickness wood samples are well predicted. Trend of predicted curve is similar to that of experiments. The second peak from the prediction is a little later than experiment, which is similar to MLR prediction. From the comparison of 10 mm thickness sample, predicted CO release rate have the same trend with experiments, showing a single peak. But predictions are higher than experimental data. Time to peak CO release rate is a little later than peak MLR. This is because time is needed for transportation inside wood slab before exhaustion to the air.

Figure 6 shows comparisons of CO release rate between prediction and experiment under 50 kW/m^2 heat flux. It is noticed that the predictions fit very well with experiments. Two peaks can be observed from CO release rate curve. The first one is before ignition. Experimental results [12,13] showed a sharp decrease of CO release rate shortly after ignition and a second peak near the end of the experiment. So in this model, it is assumed that the new produced CO during the presence of visible flame change into CO_2 immediatelyafter production. From both modeling and experiment, a sharp decrease of CO release rate was observed after ignition. But CO release didn't disappear immediately as accumulative CO inside wood slab keep flowing out through the surface by diffusion. The second peak happens after flameout. This may be because of the absence of visible flame. Oxidation reaction of CO may take slower without visible flame, resulting in an increase of CO release rate. And CO release rate will decrease until no more CO will be produced when virgin wood and char will have been run out.

Figure 7 shows comparisons of CO release rate between prediction and experiment under 75 kW/m^2 heat flux. It is observed that CO release rate are well predicted before flameout. However, predictions are much higher than experiments after flameout. In the model, it is assumed that flameout happens when the mass of solid phase is equal to the mass of produced char by consuming all the virgin wood. The difference between modeling and experiments may be because of the prediction of flameout. Char yield would decrease much under high external heat flux and this approach cannot accurately

predict flameout time under high external heat flux. Unfortunately, no empirical model has been found to predict flameout time under different external heat flux. Modeling results can be improved when this kind of empirical models will be developed.

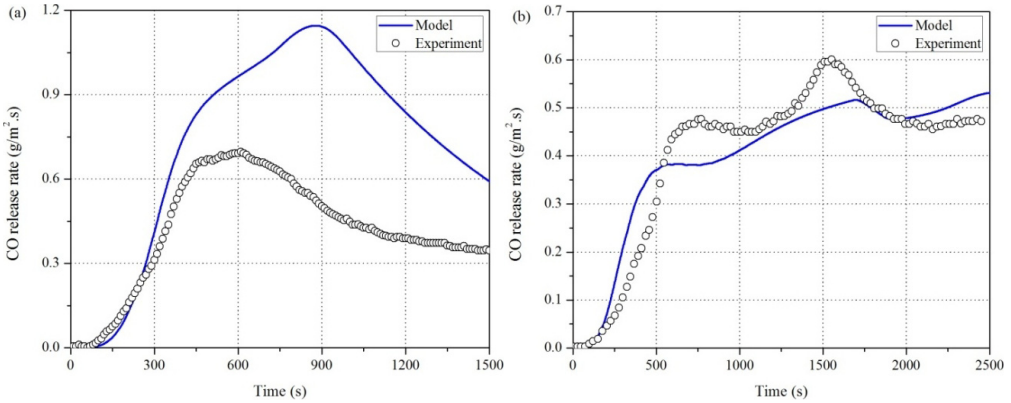

Fig. 5. Comparisons of CO release rate between prediction and experiment under 25 kW/m^2 heat flux for: (a) 10 mm thickness and (2) 20 mm thickness.

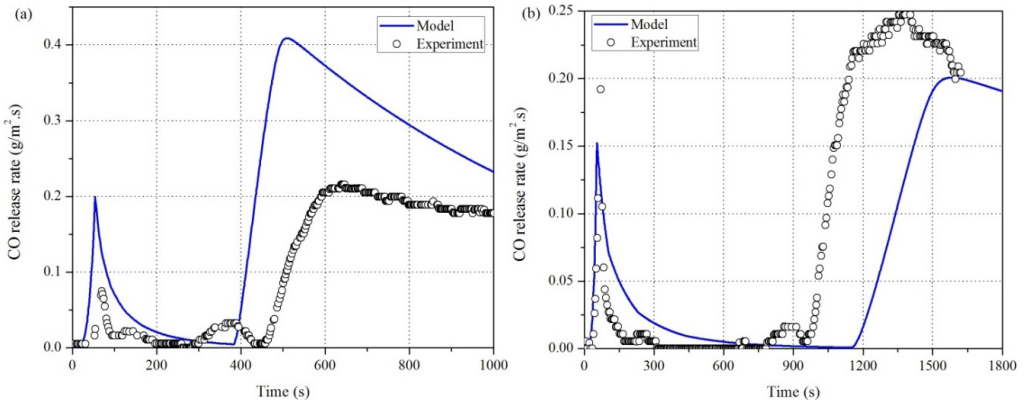

Fig. 6. Comparisons of CO release rate between prediction and experiment under 50 kW/m^2 heat flux for: (a) 10 mm thickness and (2) 20 mm thickness.

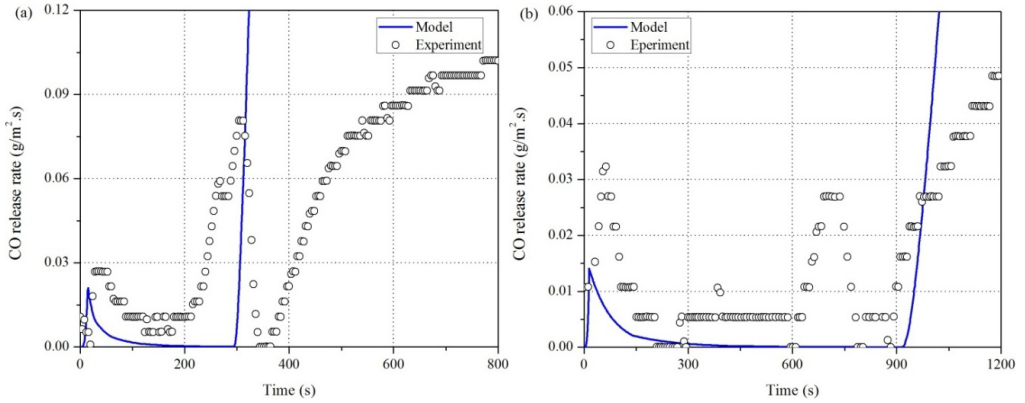

Fig. 7. Comparisons of CO release rate between prediction and experiment under 75 kW/m^2 heat flux for: (a) 10 mm thickness and (2) 20 mm thickness.

After comparing the predictions of CO release rate with experiments, it is noticed that CO release rate can be well predicted by this model. For CO release rate under different external heat flux, it is assumed that the new produced CO during the presence of visible flame change into CO_2 immediately after production. For the time period before ignition or after flameout, CO yields of each reaction are considered constant even under different external heat flux. Carbon monoxide release rate under different external heat flux can be well predicted by this approach.

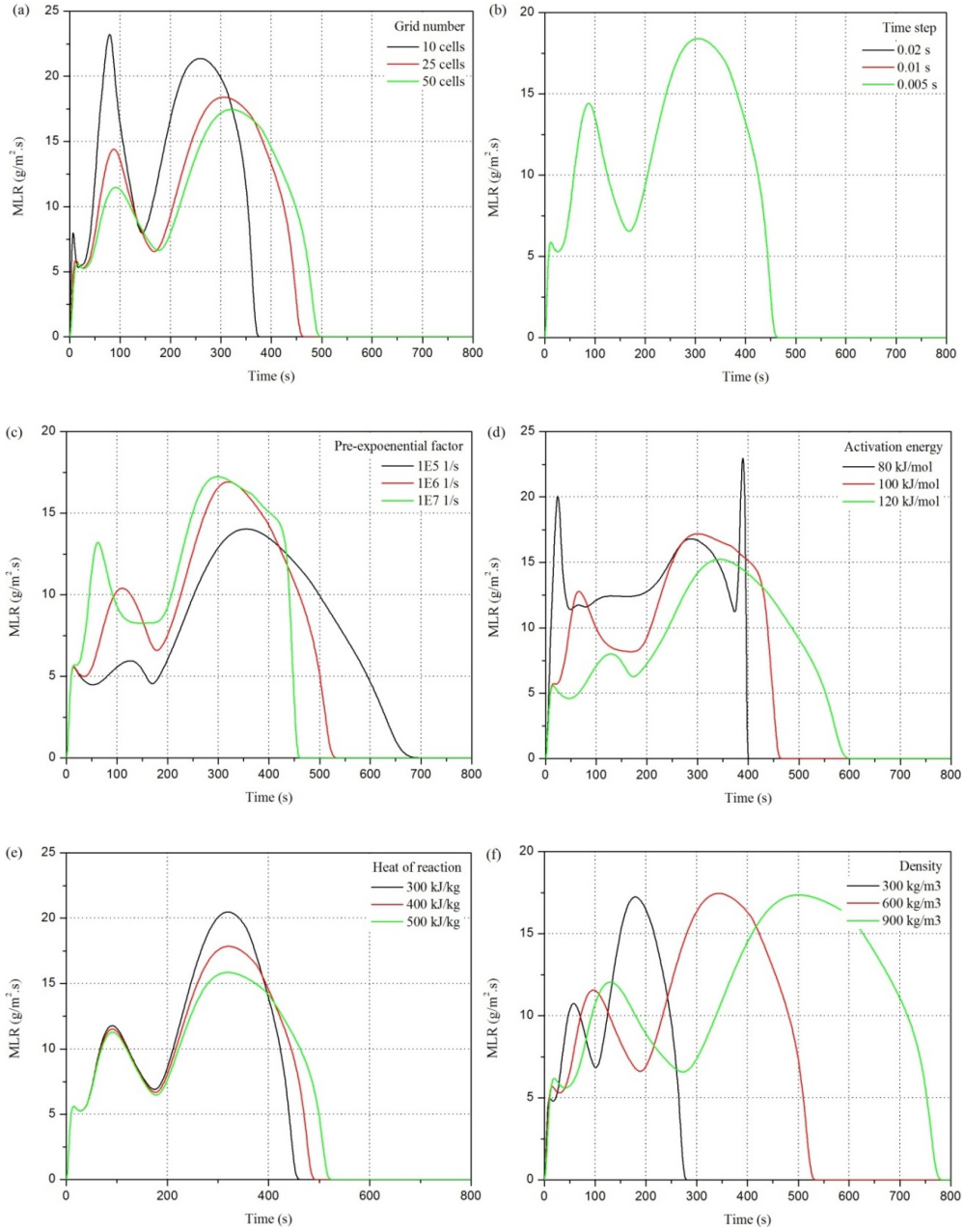

Fig. 8. Sensitivity analysis of input parameters: (a) grid number; (b) time step; (c) pre-exponential factor of virgin wood; (d) activation energy of virgin wood; (e) heat of reaction of virgin wood; and (f) wood density.

4. Sensitivity analysis of modeling input

To analyze sensitivity of modeling input, 10 mm thickness wood samples under 50 kW/m^2 external heat flux were chosen. Fig. 8 shows sensitivity analysis of modeling input parameters, such as grid number, time step, activation energy, pre-exponential factor and heat of reaction of virgin wood, and wood density. It is noticed that grid number, time step, heat or reaction of virgin wood decomposition have little influence to the MLR data. But the MLR predictions are sensitive to some parameters, such as pre-exponential factor, activation energy and wood density.

As explicit formulation was adopted to solve the equations, time step must meet the requirement that: $\Delta\bar{t} < 0.5[\min(\Delta\bar{x})]^2$. To meet the requirement, time step should be small enough. As shown in the figure, it is noticed that the time step have no influence to the modeling results when it is smaller than 0.02 s. Moreover, predicted results are affected only a little when the grid numbers are larger than 25 cells.

Modeling results are sensitive to pre-exponential factor and activation energy. For pre-exponential factor, the second peak increases considerably when it changes from 1×10^6 to 1×10^7 1/s. And MLR predictions increase with a lower activation energy.

Heat of reaction has little effect to the first stage of MLR. MLR data in the second stage decrease with a higher heat of reaction. The MLR predictions are also postponed with a higher density. Time to peak increases from about 180 to 500 s when wood density increases from 300 to 900 kg/m^3.

5. Applications of modeling

5.1. Shrinkage

Figure 9 shows the predicted shrinkage of different thicknesses wood samples under external heat flux. In this model, volume shrinkage is assumed to be related to mass loss individually. Volume shrinkage stops when no mass loss is registered. Mass loss is due to two pyrolysis reactions: virgin wood changes into char, and char changes into ash. When all the char change into ash, there will be no more mass loss.

Previous studies [14-18] have stated that wood shrinkage happens during drying process. Water evaporation process, transportation processes of water inside wood slab can be predicted by this model as well. So this model also can be used to predict volume shrinkage of wood slabs during drying process.

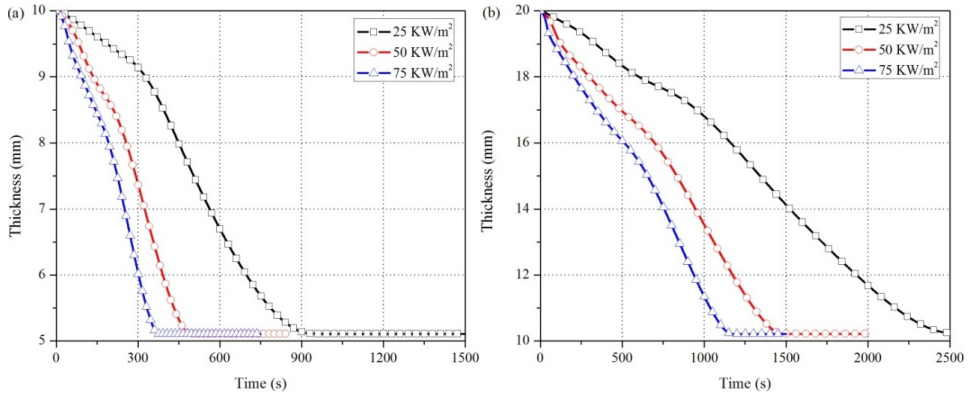

Fig. 9. Shrinkage of woods under different external heat flux for: (a) 10 mm thickness and (b) 20 mm thickness.

5.2. Water transport

Figure 10 shows contours of water transport flux of different thicknesses wood slabs under external heat flux. In these contours, *X* direction represents the time, and *Y* direction shows the depth inside wood slab. Values of transport flux are represented by color, and the range of color bar is 0-0.05 g/m^2 s.

Water transport process inside wood slab lasts a short time period when they are positioned under external heat flux. Inside the wood slab, water evaporation and transport process take place at the same time. Transport process stops when no liquid water exists inside wood slab. From these figures, it is noticed almost all the water transport last less than 300

seconds. And time period decreases with a thinner thickness or a higher external heat flux.

From Fig. 10, it is observed that water transport flux increases when temperature is rising. This is because diffusive force increases when more liquid water change into water vapor under higher temperatures. As external heat penetrates into deep depth, transport flux at the deep depth then start to increase. The transport flux at deep depth grows much quickly with a higher external heat flux.

Water transport flux seems to increase faster with thin samples. Increasing trend of transport flux at deep depth becomes much slowly with thick samples. This may be because temperature at depth increases much drastically inside a thin sample. And diffusive force caused by temperature difference then provides the impetus to drive out the water.

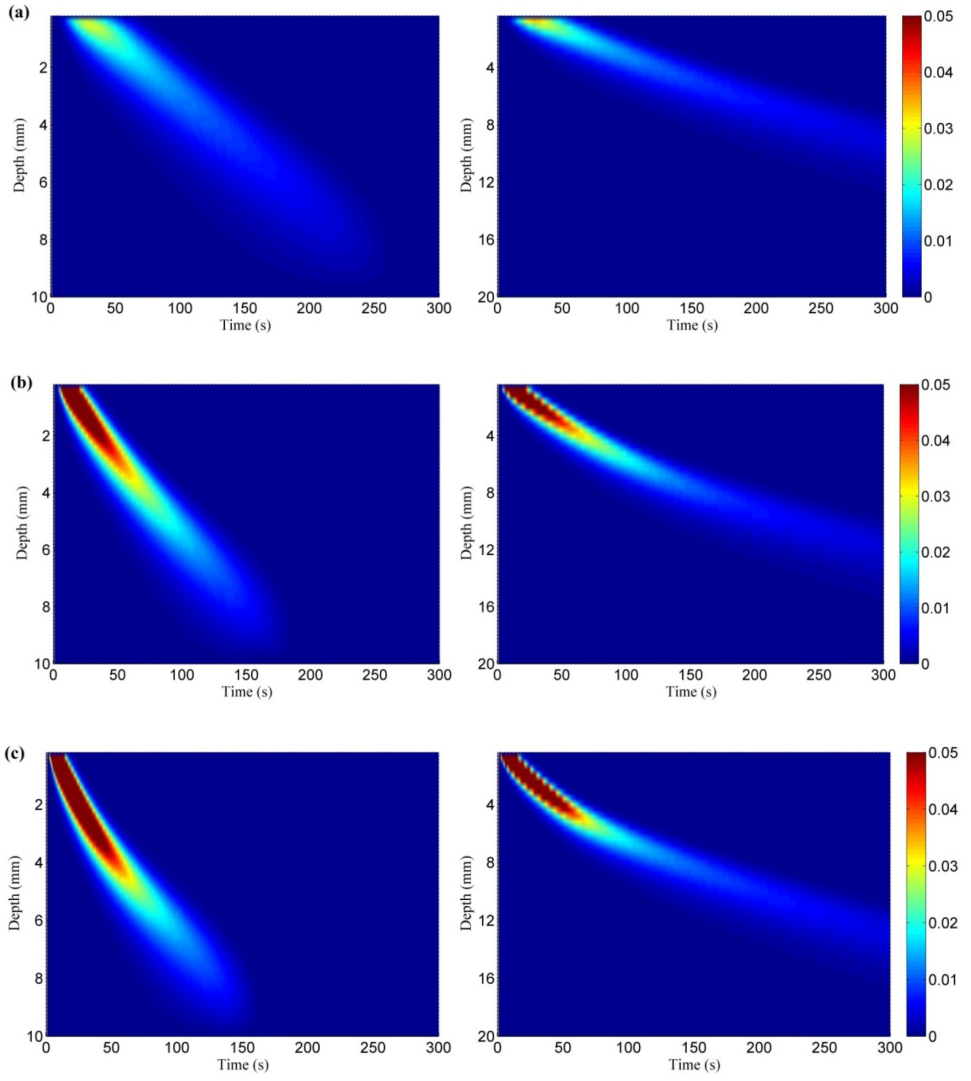

Fig. 10. Water transport flux contours under different external heat flux: (a) 25 kW/m^2; (b) 50 kW/m^2 and (c) 75 kW/m^2. Three figures in the left column are for 10 mm thickness samples, and figures in the right column are for 20 mm thickness samples.

5.3. CO transport

Figure 11 shows contours of CO transport of different thicknesses wood samples under different external heat flux. Values of transport flux are also represented by color. And the range of color bar is 0-2 g/m^2 s.

It is noticed from figures that peak CO transport flux is not at the surface but below the half depth of whole wood slab. In the model, it is assumed that all the new produced CO during the presence of visible flame change into CO_2 after production. Ignition time becomes shorter with a higher external heat flux. As transport flux of CO before flameout is very small, it is hard to be seen in the contours. Flameout time is assumed to happen when the mass of solid phase is equal to the mass of produced char by consuming all the virgin wood. With a higher external heat flux, pyrolysis reaction of virgin wood and char take place much quickly. Then flameout happens much earlier. So it is noticed from the figures that the transport process begins earlier with a higher external heat flux.

From Fig. 11, it is also observed that transport flux increases much dramatically with a thinner thickness. This may be because more heat can be absorbed for a unit mass of virgin wood under the same external heat flux. A higher diffusive force would exist as more CO is produced during pyrolysis reactions.

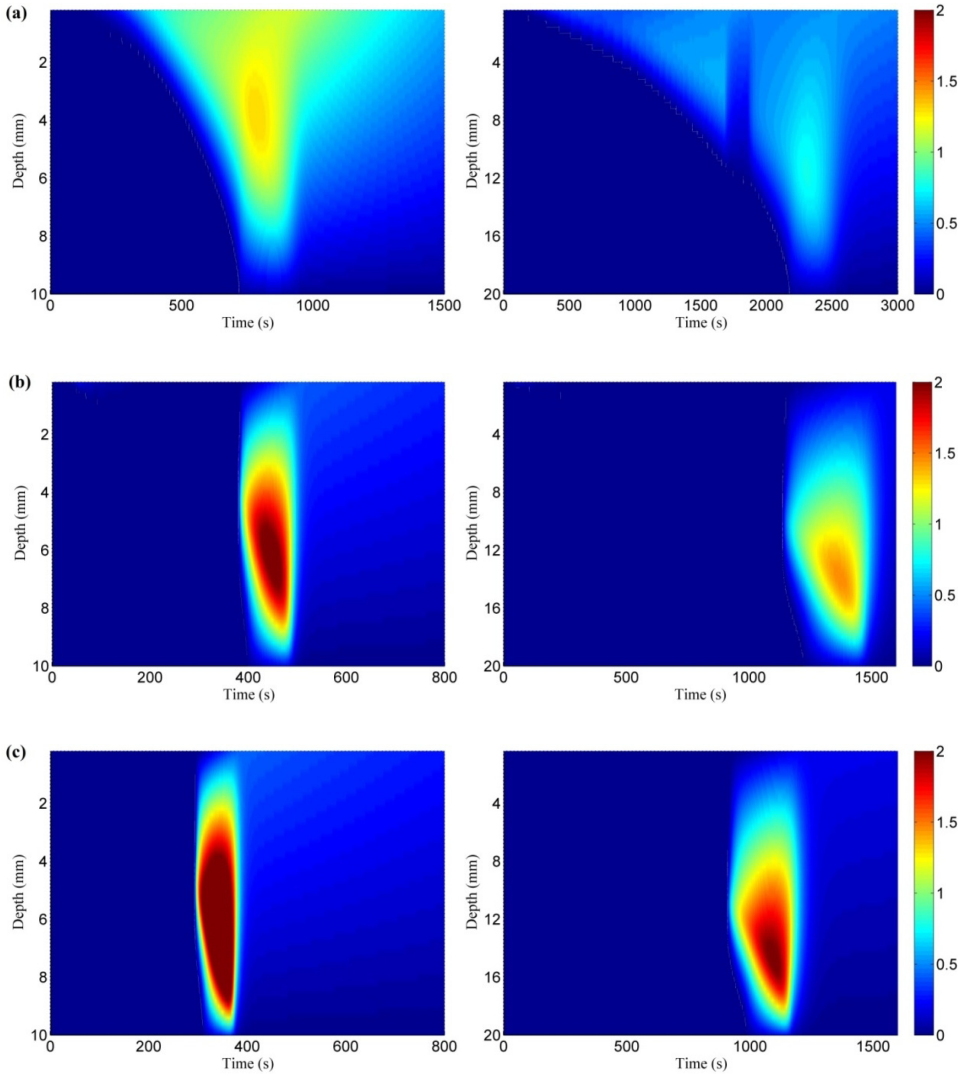

Fig. 11. CO transport flux contours under different external heat flux: (a) 25 kW/m^2; (b) 50 kW/m^2 and (c) 75 kW/m^2. Three figures in the left column are for 10 mm thickness samples, and figures in the right column are for 20 mm thickness samples.

6. Conclusions

In this two-part study, a one-dimensional model to predict CO of woods under external heat flux was developed. From the comparisons between modeling and experiment, it is noticed that MLR and CO release rate of woods under different moisture contents and external heat flux can be well predicted by this model. For CO release rate under different external heat flux, it is assumed that the new produced CO during the presence of visible flame change into CO_2 immediately after production. For time period before ignition or after flameout, CO yields of each reaction are considered constant even under different external heat flux. This will expand the applications of this model as limited experimental data of CO yields under various external heat flux. Carbon monoxide release rate of woods under different external heat flux can be well predicted by this approach. This model intends to provide a practical tool to predict toxic gases of combustible materials under fire conditions.

Besides the prediction of CO, fire processes such as water evaporation, volume shrinkage, transport of liquid water and gas volatiles also can be predicted by this model. To improve modeling accuracy, temperature and moisture dependent thermal properties are used for modeling input. Three reactions are considered in this model, such as water evaporation reaction, oxidation reactions of virgin wood and char.

Transport processes of liquid water and gas volatiles inside wood slab can also be described by this model. From the modeling results, it is noticed that water transport process inside wood slabs lasts a short time period, and the time period decreases with a thinner thickness or a higher external heat flux. It is observed from predictions that peak CO transport flux are not at the surface but below the half depth of whole wood slab, and transport flux increases much dramatically with a thinner thickness.

References

[1] Li, X. R., Koseki, H., Momota, M., 2006. Evaluation of Danger from Fermentation-induced Spontaneous Ignition of Wood Chips, Journal of Hazardous Materials 135, p. 15.
[2] Shi, L., Chew, M. Y. L., 2012. Influence of Moisture on Autoignition of Woods in Cone Calorimeter, Journal of Fire Sciences 30, p. 158.
[3] Shi, L., Chew, M. Y. L., 2012. Experimental Study of Woods under External Heat Flux by Autoignition: Ignition Time and Mass Loss Rate, Journal of Thermal Analysis and Calorimetry 111, p. 1399.
[4] Blijderveen, M. V., Gucho, E. M., Bramer, E. A., Brem, G., 2010. Spontaneous Ignition of Wood, Char and RDF in a Lab Scale Packed Bed, Fuel 89, p. 2393.
[5] Wang, Y. F., Yang, L. Z., Zhou, X. D., Dai, J. K., Zhou, Y. P., Deng, Z. H., 2010. Experiment Study of the Altitude Effects on Spontaneous Ignition Characteristics of Wood, Fuel 89, p. 1029.
[6] Tahsini, A. M., Farshchi, M., 2010. Numerical Study of Solid Fuel Evaporation and Auto-ignition in a Dump Combustor, Acta Astronautica 67, p. 774.
[7] Mitchell, P., 2011. Methods of Moisture Content Measurement in the Lumber and Furniture Industries, www.ces.ncsu.edu/.
[8] Fire Testing Technology Limited. User's Guide for the Cone Calorimeter, Fire Testing Technology Limited, West Sussex, UK, 2001.
[9] Staggs, J. E. J., 2005. Savitzky-Golay Smoothing and Numerical Differentiation of Cone Calorimeter mass Data, Fire Safety Journal 40, p. 493.
[10] Luo, J. W., Ying, K., Bai, J., 2005. Savitzky-Golay Smoothing and Differentiation Filter for Even Number Data, Signal Processing 85, p. 1429.
[11] Janssens, M., Douglas, B., 2004. Wood and Wood Products, Handbook of Building Materials for Fire Protection. McGraw-Hill, New York, pp. 7.1.
[12] Shi, L., Chew, M. Y. L., 2012. Experimental Study of Carbon Monoxide for Woods under Spontaneous Ignition Condition, Fuel 102, p. 709.
[13] Mulholland, G., Twilley, W., Babrauskas, V., Janssens, M., Yusa, S., 1991. "The Effect of Oxygen Concentration on CO and Smoke Produced by Flames," Fire Safety Science - Proceedings of the 3rd International Symposium, International Association for Fire Safety Science, pp. 585-594.
[14] Moutee M., Fortin Y., Fafard M., 2007. A Global Rheological Model of Wood Cantilever as Applied to Wood Drying, Wood Science and Technology 41, p. 209.
[15] Didriksen, H., Nielsen, J. S., 2002. A Simulation Tool for the Wood Drying Process, Computer Aided Chemical Engineering 10, p. 469.
[16] Turner, I. W., 1996. A Two-dimensional Orthotropic Model for Simulating Wood Drying Processes, Applied Mathematical Modelling 20, p. 60.
[17] Sand, U., Sandberg, J., Larfeldt, J., Fdhila, R. B., 2008. Numerical Prediction of the Transport and Pyrolysis in the Interior and Surrounding of Dry and Wet Wood log, Applied Energy 85, p. 1208.
[18] Larfeldt, J., Leckner, B., Melaaen, M. C., 2008. Modelling and Measurements of Drying and Pyrolysis of Large Wood Particles, Progress in Thermochemical Biomass Conversion, pp. 1046.